



## 1 Source apportionment of PM<sub>2.5</sub> in Shanghai based on hourly 2 molecular organic markers and other source tracers

3 Rui Li<sup>a+</sup>, Qiongqiong Wang<sup>b+</sup>, Xiao He<sup>c</sup>, Shuhui Zhu<sup>c,d</sup>, Kun Zhang<sup>a</sup>, Yusen Duan<sup>e</sup>, Qingyan Fu<sup>e</sup>,  
4 Liping Qiao<sup>d</sup>, Yangjun Wang<sup>a</sup>, Ling Huang<sup>a</sup>, Li Li<sup>a\*</sup>, and Jian Zhen Yu<sup>b,c\*</sup>

5 <sup>a</sup>School of Environmental and Chemical Engineering, Shanghai University, Shanghai, 200444, China

6 <sup>b</sup> Department of Chemistry, <sup>c</sup> Division of Environment and Sustainability, Hong Kong University of Science and  
7 Technology, Hong Kong, China

8 <sup>d</sup>State Environmental Protection Key Laboratory of the Cause and Prevention of Urban Air Pollution Complex, Shanghai  
9 Academy of Environmental Sciences, Shanghai, 200233, China

10 <sup>e</sup>Shanghai Environmental Monitoring Centre, Shanghai, 200235, China

11

12 <sup>+</sup>*These two authors contributed equally to this work.*

13 <sup>\*</sup>*Correspondence to:* Li Li (Lily@shu.edu.cn) and JianZhen Yu (jian.yu@ust.hk)

### 14 Abstract

15 Identification of various sources and quantification of their contributions are a necessary step to formulating scientifically  
16 sound pollution control strategies. Receptor model is widely used in source apportionment of fine particles. However, most  
17 of the previous studies are based on traditional filter collection and lab analysis of aerosol chemical species (usually ions,  
18 elemental carbon (EC), organic carbon (OC) and elements) as inputs. In this study, we conducted robust online  
19 measurements of a range of organic molecular makers and trace elements, in addition to the major aerosol components  
20 (ions, OC and EC), in urban Shanghai in the Yangtze River Delta region, China. The large suite of molecular and elemental  
21 tracers, together with water-soluble ions, OC and EC, provide data for establishing measurement-based source  
22 apportionment methodology for PM<sub>2.5</sub>. We conducted source apportionment using positive matrix factorization (PMF) and  
23 compared PMF solutions with molecular makers added (i.e. MM-PMF) and those without organic markers. MM-PMF  
24 identified 11 types of pollution sources, with biomass burning, cooking and secondary organic aerosol (SOA) as the  
25 additional sources identified. The three sources accounted for 4.9%, 2.6% and 14.7% of the total PM<sub>2.5</sub> mass, respectively.  
26 During the whole campaign, the secondary source is an important source of atmospheric pollution, the average contribution  
27 of secondary pollution sources is as high as 63.8% of the total PM<sub>2.5</sub> mass. Grouping different sources to secondary and  
28 primary, we note that SOC and POC contributed 45.1% and 54.9%, respectively. It is worth noting that the contribution of  
29 cooking to PM<sub>2.5</sub> mass only account for 2.6%, but it contributed to 10.7% of OC. Episodic analysis indicated that secondary  
30 nitrate was always the main cause of PM<sub>2.5</sub> pollution, while during non-episodic hours, vehicle exhaust made a significant



31 contribution. Through the application of the above-mentioned techniques to the Yangtze River Delta, more insights are  
32 gained on the sources, formation mechanism and pollution characteristics of PM<sub>2.5</sub> in this region.

### 33 **1. Introduction**

34 In recent years, with the increasingly prominent problem of air quality, more and more attention has been paid to the  
35 research of air pollution, which focuses on the study of atmospheric particulate matter (PM), especially fine particulate  
36 matter (PM<sub>2.5</sub>) (Chen et al., 2007; Zhang et al., 2009a). The study of chemical composition of atmospheric PM<sub>2.5</sub> is to help  
37 understand the source, formation mechanism, and environmental effects. PM<sub>2.5</sub> pollution reduces atmospheric visibility  
38 (Chow et al., 2004) and exposure to PM<sub>2.5</sub> is positively correlated with adverse health effects (Nel, 2005; Lippmann et al.,  
39 2009; Mimura et al., 2014; Liu et al., 2016; Jimenez et al., 2009). PM<sub>2.5</sub> in the atmosphere also affects the radiation balance  
40 on the ground by scattering or absorbing solar radiation and changing the properties of clouds, which has an impact on  
41 global climate (Foley et al., 2010; Ramanathan et al., 2001; Kanakidou et al., 2005). Therefore, PM<sub>2.5</sub> pollution has become  
42 the primary control target to improve air quality in urban environments. Studying the composition of PM<sub>2.5</sub> and identifying  
43 its sources have practical significance for the understanding of PM<sub>2.5</sub> pollution characteristics and environmental effects.

44 The analysis of the sources is of great significance for PM<sub>2.5</sub> emission reduction and pollution control (Huang et al.,  
45 2014; Wang et al., 2017). Generally, the sources of pollution can be qualitatively assessed according to presence of chemical  
46 components characteristic to specific sources. In addition, receptor models can be used to further identify and quantify the  
47 sources of atmospheric PM<sub>2.5</sub> (Hopke, 2016; Jaeckels et al., 2007; Lee et al., 2008; Sofowote et al., 2014;). Compared with  
48 other methods, Positive Matrix Factorization (PMF) (Paatero & Tapper, 1994) does not need to input the source profiles,  
49 and we can simultaneously analyze the source profiles and contributions of various sources. Hence, PMF has been widely  
50 used in the source analysis of PM<sub>2.5</sub> all over the world, for example, Beijing (Song et al., 2006; Yao et al., 2016), Shanghai  
51 (Wang et al., 2018; Wang et al., 2013; Feng et al., 2013; Feng et al., 2012; Wang et al., 2015; Wang et al., 2014; Zhao et al.,  
52 2015; Qiao et al., 2016), Hong Kong (Hu et al., 2010; Yuan et al., 2006), New York (Zhou et al., 2019; Masiol et al.,  
53 2017), and other regions (Ulbrich et al., 2009; Fang et al., 2015).

54 High time resolution measurements are inherently advantageous to the source analysis, because they are able to  
55 capture the diurnal variations of the main source activities (such as vehicle exhaust) and secondary formation processes.  
56 High time resolution data provide opportunities to study short-term source distributions. There are limited number of source  
57 apportionment studies exploring the combined high-time resolution data set including various aerosol components such as  
58 trace elements (Wang et al., 2018). Online-measurement based source apportionment studies in the past, so far, are mainly



59 based on PM<sub>1</sub> Aerodyne aerosol mass spectrometer (AMS) or Aerosol chemical speciation monitoring (ACSM) (Al-  
60 Naiema et al., 2018). AMS or ACSM provide data on ion fragments, which only retain partial information for their parent  
61 molecules. Multiple parent molecules could lead to the same fragments during the ionization process in AMS or ACSM,  
62 which introduce ambiguity in relying on fragment ions for source differentiation. Accurate quantitative monitoring of  
63 atmospheric organic matter on the molecular level is critical to source analysis.

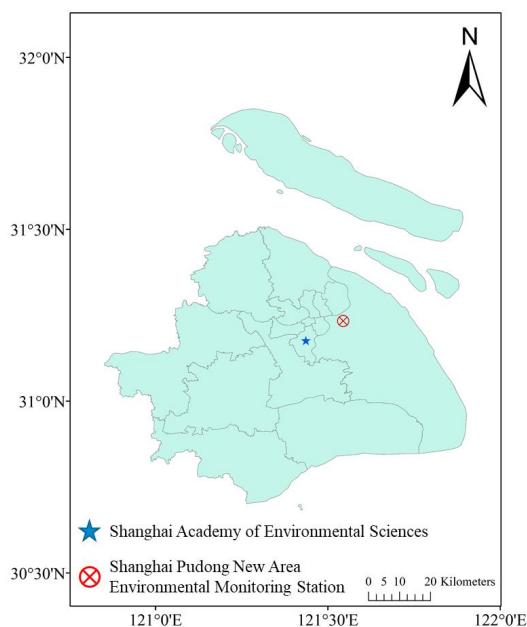
64 Shanghai is the financial center of China, with a large population and a total area of 6,340 km<sup>2</sup>. Past source  
65 apportionment studies of PM<sub>2.5</sub> in Shanghai were either based on offline filters using receptor models (Du et al., 2017;  
66 Chang et al., 2018), or emissions with numerical models (Li et al., 2015; Shu et al., 2019; Li et al., 2019; Feng et al., 2019).  
67 The past receptor modeling studies relied on chemical composition data derived from 24-h time-integrated filter samples  
68 followed by off-line laboratory analysis. The off-line nature severely limits its utility in addressing episodic pollution events  
69 and in providing data to assess emission-based model evaluation of pollution sources and regional transport. Some  
70 researchers have conducted online PM<sub>2.5</sub> source apportionment, however, previous studies were mainly using the traditional  
71 aerosol species as inputs (Wang et al., 2018). Organic matter constitutes a considerable share of PM<sub>2.5</sub>, while the online  
72 analytical techniques used in the past were not suitable for describing this fraction in full.

73 In this study, online monitoring of atmospheric PM<sub>2.5</sub> compositions, including inorganic ions, organic carbon (OC),  
74 elemental carbon (EC), trace elements and organic molecular markers, was conducted in Shanghai from November 9 to  
75 December 3, 2018. The purpose is to use the detailed high-time resolution speciation data (especially organic molecular  
76 markers) to identify the sources of PM<sub>2.5</sub> based on molecular-marker based PMF. This study gives insights into more  
77 detailed source contributions, changes of sources and effects of the air pollution control strategies.

## 78 **2. Methodology**

### 79 **2.1 Online measurement**

80 We conducted an observation for PM<sub>2.5</sub> and its major chemical compositions (including inorganic ions, OC, EC,  
81 elements, and organic tracers) from November 9 to December 3, 2018. The organic tracers were measured in Shanghai  
82 Academy of Environmental Sciences, which is a representative site for the urban city. The inorganic ions, OC/EC, and  
83 elements were measured in Shanghai Pudong Environmental Monitoring Station, which is also a typical site for the urban  
84 city. Monitoring site locations are shown in Figure 1. The two sites are 12 km apart. We combined these data in order to  
85 obtain a more comprehensive chemical characterization of the urban PM<sub>2.5</sub> air pollution situation.



86

87 **Figure 1. Locations of the two sampling sites in Shanghai, China**

88 The concentration of PM<sub>2.5</sub> was measured by an online beta attenuation particulate monitor (FH 62 C14 series, Thermo  
89 Fisher Scientific) (Qiao et al., 2014). Carbonaceous materials (OC and EC) were monitored by a semi continuous OC/EC  
90 analyzer (model RT-4, Sunset Laboratory, Tigard, OR, USA) (Nicolosi et al., 2018; Zhang et al., 2017). The water-soluble  
91 inorganic ions were measured by Monitor for Aerosols and Gases (MARGA, Model ADI 2080, Applikon Analytical B.V.)  
92 (Makkonen et al., 2012; Griffith et al., 2015). Concentrations of 22 elements in PM<sub>2.5</sub> were measured by an ambient  
93 elemental monitor (Xact 625 Ambient Continuous Multi-metals Monitor, Cooper Environmental Services, Tigard, OR,  
94 USA) using nondispersive X-ray fluorescence (XRF) analysis (Battelle, 2012; Jeong et al., 2019). Quantification of hourly  
95 speciated organic compounds were achieved using a Thermal desorption Aerosol Gas Chromatograph (TAG) (Williams et  
96 al., 2014; Zhao et al., 2013a; Isaacman et al., 2014). The operation details and data quality are described in a separate paper  
97 (Wang et al., 2019). Figure S1 shows the comparison of reconstructed and measured PM<sub>2.5</sub> mass for samples collected for  
98 this study (Wang et al., 2016; Huang et al., 2014). The meteorological parameters are from the open data at Hongqiao  
99 airport (available at <http://www.wunderground.com>).

## 100 2.2 PMF receptor model

101 PMF is a bilinear factor analysis method, which is widely used to identify pollution sources and quantify the



102 contribution of source sectors to the concentration of ambient air pollutants at receptor sites, with an assumption of mass  
103 conservation and a chemical mass balance between emission source and receptors. In this study, the Environmental  
104 Protection Agency (EPA) PMF version 5.0 (Norris et al., 2014) was applied to perform the analysis. PMF decomposes the  
105 measured data matrix,  $X_{ij}$ , into a factor profile matrix,  $f_{kj}$ , and a factor contribution matrix,  $g_{ik}$ , (Eq 1):

$$106 \quad x_{ij} = \sum_{k=1}^p g_{ik} f_{kj} + e_{ij} \quad (1)$$

$$107 \quad Q = \sum_{i=1}^n \sum_{j=1}^m (e_{ij}/u_{ij})^2 \quad (2)$$

108 In eq 1,  $X_{ij}$  is the measured ambient concentration of target pollutants;  $g_{ik}$  is the source contribution of the  $k^{\text{th}}$  factor  
109 to the  $i^{\text{th}}$  sample, and  $f_{kj}$  is the factor profile of the  $j^{\text{th}}$  specie in the  $k^{\text{th}}$  factor;  $e_{ij}$  is the residual concentration for each data  
110 point. PMF seeks a solution that minimizes an object function  $Q$  (Eq 2), based on the uncertainties of each observation  $u_{ij}$ .  
111 The user provides the  $u_{ij}$  for each data point. The selection of the best factor in this study and the error estimation diagnostics  
112 for each model result are described in the supplement information (Figure S2, Figure S3, Table S1, Table S2).

113 PMF model assumes that the quantity of the input species is conserved, and the source profile is unchanged. In order  
114 to minimize the impact of organic matter degradation on the deviation of mass conservation hypothesis, organic species  
115 with low volatility and low reactivity are selected as input. The requirement of constant source profiles is not strictly met  
116 when the receptor model is applied to measurement data covering a long duration (e.g., months or longer). However,  
117 understanding/progress can be achieved despite the non-strict adherence to the requirements of the constant source profile.  
118 The source profile parsed by PMF can be viewed as the averaged profile over the entire sampling period. In an atmospheric  
119 environment, both primary organic aerosol (POA) and secondary organic aerosol (SOA) have the problem of changing  
120 source profiles. Therefore, it is necessary and vital to obtain high time resolution data, preferably several hours for a sample  
121 of data or shorter, as an input file for PMF model. The input files in this study are hourly data and the time span of whole  
122 campaign is less than one month. As such, the source type information will not change significantly.

123 In this study, a total of 289 samples has been collected. The hourly chemical species selected as input to PMF model  
124 contain 13 elements, 4 inorganic species, the carbon component (OC and EC), organic markers (including polycyclic  
125 aromatic hydrocarbons (PAHs) and anhydro sugars, etc.), and  $PM_{2.5}$  mass concentration. Traditional PMF (PMFt, “t” refers  
126 to traditional) which include only  $PM_{2.5}$  mass, elements, inorganic ions, OC and EC as inputs, and molecular marker based-  
127 PMF (MM-PMF) (Al-Naiema et al., 2018; Wang et al., 2017; Zhang et al., 2009b) with organic markers added as inputs  
128 on the basis of above species were performed separately to do source apportionment.

129 The uncertainty of each data point is calculated according to Eq 3:



$$130 \quad u_{ij} = \sqrt{(x_{ij} \times EF)^2 + (\frac{1}{2} \times MDL)^2} \quad (3)$$

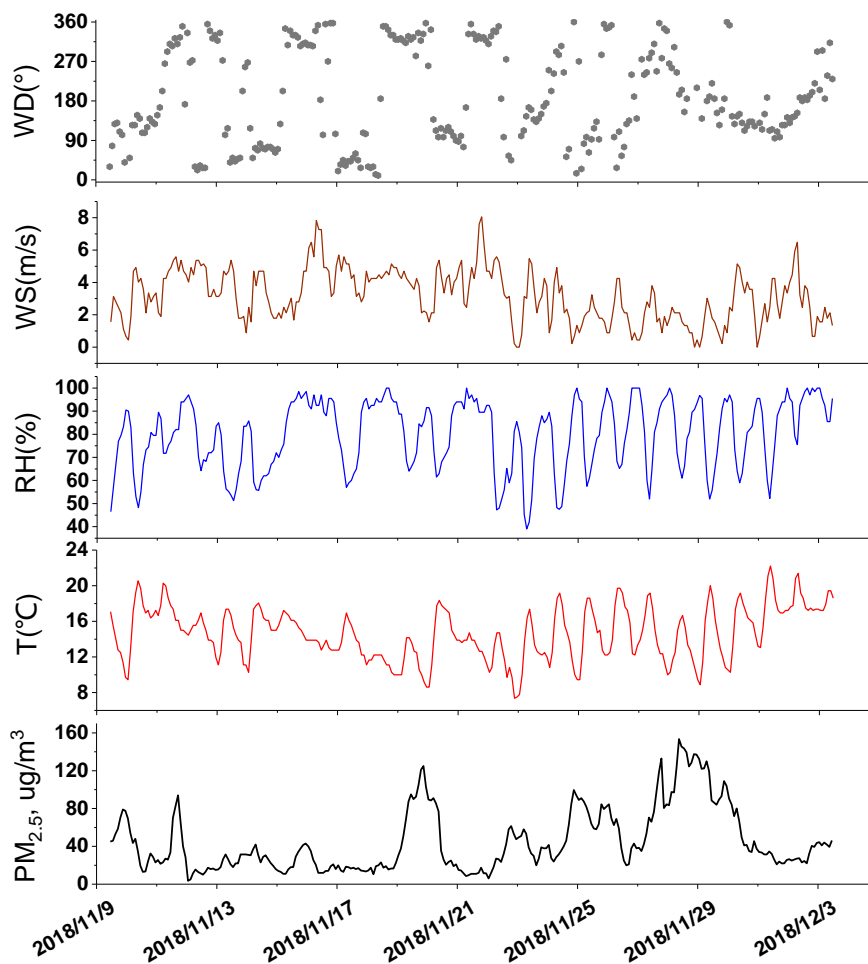
131 where MDL is the method detection limit and EF is the error fraction determined by the user and associated with the  
132 measurement uncertainty. The concentration data of species below the detection limit were replaced by 1/2 of the MDL,  
133 and the  $u_{ij}$  was calculated by 5/6 of the MDL. For the concentration data of missing species, the missing value is the  
134 geometric average value of the concentration of this species, and its  $u_{ij}$  is four times the geometric average value.

### 135 **2.3 Trajectory analysis**

136 The backward trajectory analysis is a useful tool to identify the influence of air mass path on PMF resolved  
137 sources. 36-h duration backward trajectories arriving at an altitude of 100 m above ground level (AGL) over the site were  
138 calculated using the NOAA HYSPLIT model (<https://ready.arl.noaa.gov/HYSPLIT.php>), deploying the 0.5° Global Data  
139 Assimilation System (GDAS) meteorological data. The sampling days were then classified into four clusters according to  
140 the geographical origin and movement process of the trajectories, i.e., two oceanic trajectories, and two continental  
141 trajectories.

## 142 **3. Results and discussion**

143 The pollution episodes occurred mostly in winter, due to adverse atmospheric conditions (such as more frequent  
144 stagnation of atmospheric movement) and enhanced the impact on air quality from local and regional emissions. The  
145 hourly meteorological parameters and PM<sub>2.5</sub> concentration during the monitoring time is shown in Fig. 2. The concentration  
146 levels of the major species measured are provided in Table 1. The average temperature was 14°C, the relative humidity  
147 (RH) was 79.9%, the wind speed (WS) was 3m/s during the campaign. The average PM<sub>2.5</sub> concentrations were 46.3±33.8  
148 µg/m<sup>3</sup>, with organic matter contributing to 19.6% of the total mass. Nitrate, sulfate, and ammonium contributed to 32.0%,  
149 16.5%, and 16.2% of PM<sub>2.5</sub>, respectively. Measured total elements account for 3.5% of PM<sub>2.5</sub> mass on average.



150

151

Figure 2. Time series of meteorological parameters and  $PM_{2.5}$  during the field campaign.



152 **Table 1. Measured PM<sub>2.5</sub> major components (µg/m<sup>3</sup>) used in the PMF analysis in this study**

Compound	Average	Stdev
PM <sub>2.5</sub>	46.3	33.8
Cl <sup>-</sup>	0.78	0.52
Nitrate	14.81	15.12
Sulfate	7.65	4.31
Ammonium	7.47	6.25
EC	1.59	1.13
OC	6.48	2.79
As	0.006	0.005
Ba	0.024	0.017
Ca	0.137	0.104
Cr	0.004	0.005
Cu	0.012	0.008
Fe	0.445	0.627
K	0.381	0.196
Mn	0.065	0.069
Ni	0.004	0.003
Pb	0.025	0.026
Si	0.421	0.322
V	0.0031	0.0029
Zn	0.114	0.099

153

154 **Table 2. Abundance and naming of measured organic tracers (ng/m<sup>3</sup>) used in the MM-PMF Analysis**

Naming	Grouping	Average	Stdev
PAHs252	benzo[b]fluoranthene, benzo[k]fluoranthene, benzo[e]pyrene, and benzo[a]pyrene	1.44	1.43
PAHs276	benzo[ghi]perylene, and indeno[1,2,3-cd]pyrene	0.559	0.529
C <sub>6-8</sub> DICAs	Adipic acid, Pimelic acid, and Suberic acid	17.45	18.46
C <sub>9</sub> -acids	9-Oxononanoic acid, and Azelaic acid	9.25	6.46
SFAs	Palmitic acid, and Stearic acid	71.57	60.86
Mannosan		1.54	1.51
Levogluconan		45.91	39.17
OHBAs	3-hydroxybenzoic acid, and 4-hydroxybenzoic acid	1.05	0.85
α-pinT	Pinic acid, and 3-methyl-1,2,3-butanetricarboxylic acid	21.05	19.22
DHOPA	2,3-dihydroxy-4-oxopentanoic acid	3.93	4.92
Phthalic acid		9.13	10.28

155 **3.1 PM<sub>2.5</sub> source apportionment**

156 In this study, PMF source analysis was conducted in two scenarios. They were MM-PMF with organic tracers and





157 PMFt without organic tracers included and the results were compared in detail. The abundance and nomenclature of the  
158 organic tracers used are shown in Table 2. The priority input species for PMF analysis are those with high abundance and  
159 characteristics of different sources, especially organic compounds with lower volatility and lower reactivity were selected  
160 as input for MM-PMF. Highly correlated organic species ( $R > 0.8$ ), indicating common sources, are clustered together to  
161 reduce the number of species and to avoid collinearity problems in MM-PMF (Wang et al., 2017).

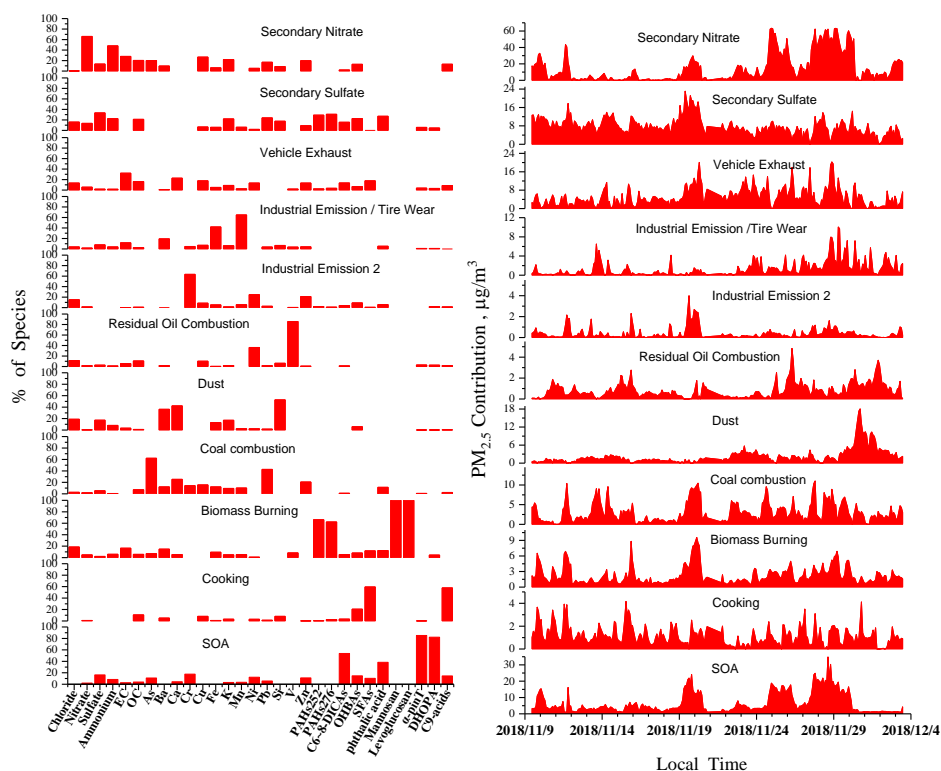
### 162 3.1.1 MM-PMF results

163 In PMF, the optimal number of factors is a compromise between identifying factors with the best physical explanations  
164 and achieving a sufficiently good fit for all species. In PMF solutions of too few factors, different sources are combined  
165 together, the resolved sources cannot fully explain the individual species; while too many factors may split one source into  
166 multiple uninterpretable factors. Initially, 7 to 14 factors were tested, and the final factor numbers were determined by  
167 examining the change in  $Q/Q_{exp}$ . Finally, the 11-factor solution for MM-PMF was selected as it gave the most reasonable  
168 factor profiles (Figure S2). Table S1 shows the summary of error estimation diagnostics from BS, DISP and BS-DISP for  
169 MM-PMF. The summary of the model performance for individual input species for the 11-factor solution in MM-PMF are  
170 given in Table S3. Nevertheless, the base run results still have certain degrees of factor mixing. As the source specific  
171 tracer compounds have similar temporal variations and the diversity of species components contained in the source,  
172 chloride, sulfate and certain metal elements were found in different PMF-resolved profiles.

173 Factor recognition was based on the highest loaded species of each factor. The factor profiles of the 11-factor solution  
174 are shown in Fig. 3. Secondary nitrate factor (F1) was identified by high concentrations of nitrate and ammonium, the  
175 distribution of ammonium and nitrate in F1 is 48.1% and 66.2% respectively. The secondary sulfate factor (F2) is  
176 characterized by the highest loading of sulfate (35.3%). In addition, ammonium in the secondary sulfate factor distribution  
177 ranks the second among the eleven factors, less than F1. A small amount of organics acids and PAHs also appear in the two  
178 factors. OC contribution from the secondary sulfate, secondary nitrate, and SOA factors were assumed as secondary OC  
179 (SOC), whereas OC from the other factors was assumed to be primary OC (POC). The secondary sulfate factor contributes  
180 the most to SOC, which can be seen from the correlation of the respective species with OC. Percentage contribution of  
181 various source factors to  $PM_{2.5}$  and to OC based on MM-PMF show in Fig.4. F1 and F2 contributed 33.5% and 15.6% to  
182 total  $PM_{2.5}$  mass, respectively. The SOC associated with secondary nitrate and sulfate factors accounted for  $2.68 \mu\text{g}/\text{m}^3$   
183 (41.3%) on average across the whole observation period. The diurnal variation of F1 showed much higher contributions at  
184 nighttime; while for F2, no obvious diurnal contrast was observed. F1 has the medium and highest correlation with  $NO_x$



185 (R = 0.54) and CO (R = 0.79) while F2 showed moderate correlations with SO<sub>2</sub> (R = 0.32) and CO (R = 0.36) (Table S4).  
 186 These results suggest that F1 may represent condensation of oxidation products of local emissions in the nighttime plus  
 187 regional transportation. Sun et al. (2006) observed increased sulfate formation under high RH in winter in urban city.  
 188 During the observation period, the RH is high during the day and night, and the daytime temperature is higher than the  
 189 nighttime. Therefore, the combined effects of aqueous phase oxidation and daytime photochemical reactions, leading to  
 190 the not obvious daily variation of the secondary sulfate factor.



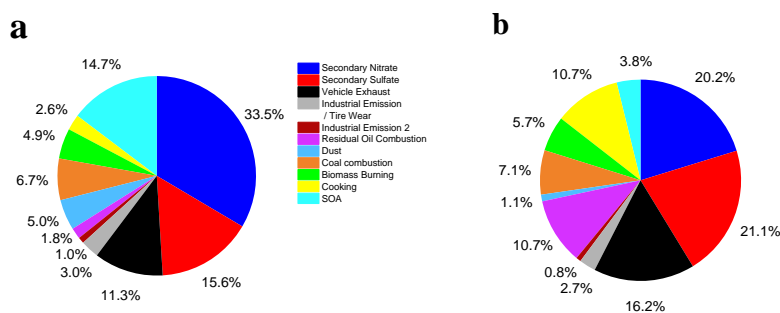
191

192 **Figure 3. Resolved factor profiles (left) and factor contributions (right) in eleven-factor solution in MM-PMF**

193 The third factor (F3) has a high abundance of EC, OC, Ca, Cu and also contains some organic tracers (PAHs and  
 194 organic acids, etc.), contributing to 11.3% of the total PM<sub>2.5</sub> mass on average. The source of vehicle exhaust contributes the  
 195 most to POC, accounting for 16.2% to OC. Vehicle exhaust is an important source for carbonaceous species, the presence  
 196 of Cu may originate from both fuel/lubricant combustion and brake abrasions (Adachi and Tainosho, 2004; Pant and  
 197 Harrison, 2013), and the element Ca may be derived from road dust. The influence of vehicle exhaust on this factor is  
 198 supported by the peak hours at 7:00-9:00 am and 5:00-7:00 pm in daily variation (Fig. 5). In addition, the high correlation



199 with NO<sub>x</sub> (R=67) and CO (R=58) indicate that vehicle exhaust have a significant impact on this factor. The higher nighttime  
200 than daytime contribution of this factor may suggest influence from the planetary boundary layer height variation. In the  
201 daytime, higher boundary height leads to more vertical mixing of the pollutants and facilitates dispersion, while the stagnant  
202 nighttime atmosphere easily accumulates pollutants (Liu and Liang, 2010).

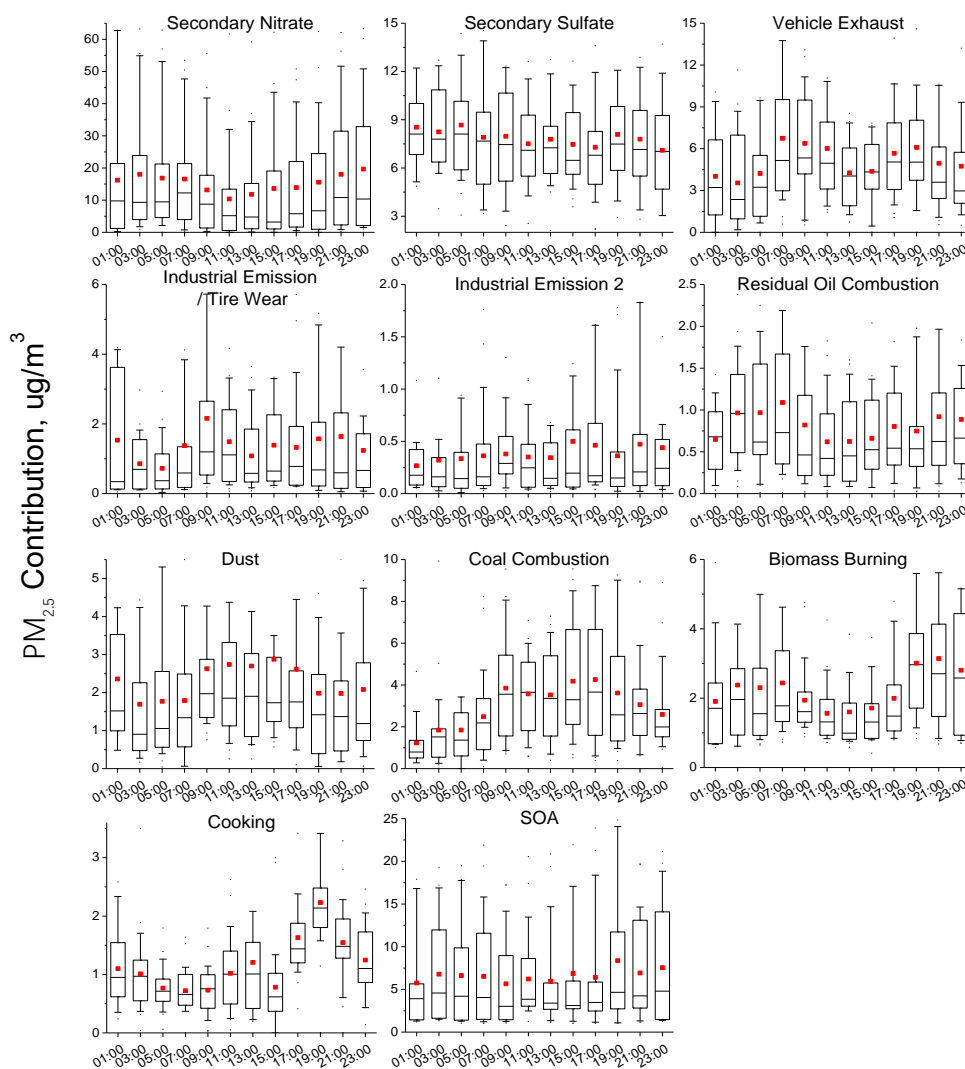


203  
204 **Figure 4. Percentage contribution of various source factors to PM<sub>2.5</sub> (a) and to OC (b) based on MM-PMF.**

205 Factor 4 contains high loads of Fe and Mn as source tracers, in addition, it contains Ba as well. Most of these metal  
206 elements come from industries related to steel production. Although metallic elements are not exclusive tracers of industrial  
207 emissions, there are no other characteristic elements or compounds to track industrial emissions. In addition, the diurnal  
208 variation of F4 is similar to that of F3, which may be due to the tire wear in the morning and evening peak. Manganese-  
209 ferro, Zn, Cu and other elements have also been reported to be related to tire wear (Pant and Harrison, 2013), and Wang et  
210 al. (2018) also revealed this in their research on online data. While F2 showed moderate correlations with SO<sub>2</sub> (R = 0.52),  
211 CO (R=0.35) and NO<sub>x</sub> (R=49), therefore, F4 is considered as the industrial and Vehicle emission source. The factor  
212 contribution to total PM<sub>2.5</sub> mass and OC was minor, only 3.0% and 2.7%, respectively. Analysis of membrane samples in  
213 the area did not reveal this phenomenon (Du et al., 2017; Huang et al., 2014; Qiao et al., 2016), suggesting the benefit of  
214 the online high-resolution measurement. The fifth factor (F5) is characterized by high concentrations of Cr and Ni, which  
215 are often used in industrial processes such as plating, tanning, and metallurgy (Karar et al., 2006; Borai et al., 2002). This  
216 factor showed best correlation with CO (R = 59). No diurnal variation was observed. The factor contribution to total PM<sub>2.5</sub>  
217 and OC mass were minor, only 1.0% and 0.8%. The residual oil combustion factor (F6) was identified with V and Ni as  
218 tracers, of which V is often used as a tracer for residual oil combustion. The contribution of this factor mainly comes from  
219 ship transportation (Zhao et al., 2013b). The diurnal contribution at night was greater than that during daytime. The factor,  
220 residual oil combustion, were minor contributors to PM<sub>2.5</sub>, accounting for 1.8%, but the contribution (10.7%) of this factor  
221 to OC is not negligible. The dust factor (F7) was distinguished by crustal elements Ca, Si, and Ba. The diurnal variation of



222 this factor showed a broad peak during the daytime, and negative correlation with RH ( $R=-0.26$ ), suggesting an influence  
223 from meteorological conditions. The factor (dust) contribution to total  $PM_{2.5}$  and OC mass were 5.0% and 1.1%,  
224 respectively.



225

226 **Figure 5.** Diurnal variation of various source factors based on MM-PMF. (25<sup>th</sup> and 75<sup>th</sup> percentile boxes, 10<sup>th</sup> and 90<sup>th</sup>  
227 percentile whiskers; lines inside the boxes represent the hourly median and the red points represent the hourly mean)

228 The coal combustion factor (F8) contains high loading of metals As and Pb, accounting for 6.7 % of  $PM_{2.5}$  mass on  
229 average and 7.1% to OC, it is mostly associated with coal combustion (Chen et al., 2013). Good correlations with  $SO_2$  (R



230 = 59) and CO ( $R = 56$ ) further support the identification of this factor. Based on analysis of MM-PMF, there is no specific  
231 organic tracers such as PAHs present in the source. The results are different from those of Wang et al. (2017) and Yu et al.  
232 (2016), which are related to regional differences in source classes.

233 The F9 and F10 were resolved, namely, biomass burning identified by levoglucosan and mannosan; cooking aerosol  
234 by SFAs (Palmitic acid, and Stearic acid) and C<sub>9</sub>-acids (9-oxononanoic acid, and azelaic acid). Levoglucosan is uniquely  
235 emitted by biomass burning activities (Engling et al., 2006; Feng et al., 2013). Using Levoglucosan to indicate biomass  
236 burning may avoid the ambiguity of using K to determine the biomass burning source, which improves the accuracy of  
237 source analysis. This factor, contributed 4.9% and 5.7% of total PM<sub>2.5</sub> and OC mass on average, respectively. In addition,  
238 biomass burning contains high-loading of five-ring and six-ring PAHs that are considered to be derived from a mixed  
239 combustion source (including coal combustion, biomass burning, etc.). It is worth noting that the contribution of cooking  
240 to PM<sub>2.5</sub> mass only account for 2.6%, but it contributed 10.7% to OC. In addition, by analyzing the diurnal variation of  
241 biomass burning and cooking, the biomass burning emission at night is greater than at daytime, while cooking has an  
242 obvious peak value during 5:00-9:00 pm, which is consistent with the local dining consumption habits in Shanghai.

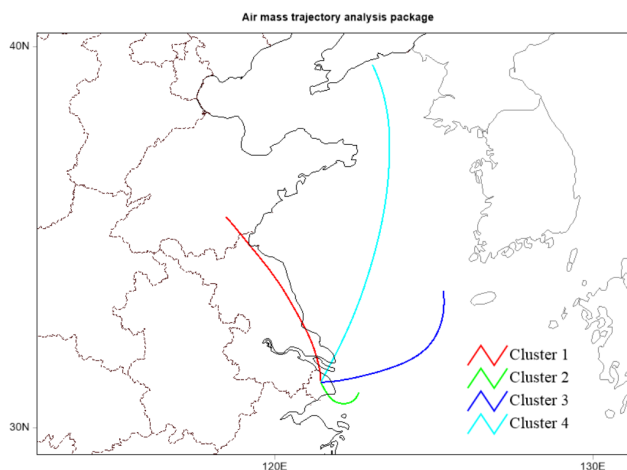
243 SOA was identified by toluene SOA tracer (2,3-dihydroxy-4-oxopentanoic acid),  $\alpha$ -pinene SOA tracers (pinic acid  
244 and 3-methyl-1,2,3-butanetricarboxylic acid) and phthalic acid. It is a major source of PM<sub>2.5</sub>, accounting for 14.7%. SOC  
245 from the SOA factor accounted for 0.25  $\mu\text{g}/\text{m}^3$  (3.8%) on average to OC. SOA related to toluene was considered as  
246 anthropogenic SOA, and SOA containing pinic acid was considered as biogenic SOA. It was found that there was a similar  
247 daily changes between SOA and secondary nitrate factor, indicating some commonality in their formation processes. Many  
248 studies have documented the enhancement of biogenic SOA production by anthropogenic species through creating a more  
249 acidic environment in the aerosol (Jang et al., 2002; Wang et al., 2017).

250 Overall, the source apportionment results showed that secondary sources accounted for 63.9% of the total PM<sub>2.5</sub> mass  
251 from MM-PMF, and the contribution of secondary nitrate to PM<sub>2.5</sub> was greater than that of secondary sulfate. SOA is the  
252 third largest source of PM<sub>2.5</sub>, followed by vehicle exhaust, which is the largest source of primary sources. The SOC  
253 associated with secondary nitrate, secondary sulfate and SOA factors accounted for 45.1% on average of the total OC mass  
254 across all the study period. The high loading of SOC in the secondary nitrate and sulfate factor compared with the SOA  
255 factor may indicate the potential mix of the SOA in secondary sulfate factor due to the limited organic tracers included.  
256 POC accounts for 3.55  $\mu\text{g}/\text{m}^3$  (54.8%) of the total OC. And vehicle exhaust contributes the most to POC. MM-PMF gives  
257 more detailed allocation of PM<sub>2.5</sub> to more accurate source factors.



### 258 3.1.2. Back Trajectory Analysis of MM-PMF-Resolved Sources

259 Previous studies based on source models have shown the importance of regional transportation and local emissions to  
260 Shanghai haze events. Wang et al. (2014) identified two types of haze events in November 2010: local emission plays a  
261 dominant role in the case of weak wind ( $WS < 0.5\text{ m/s}$ ), while in the case of stroke ( $\sim 2\text{ m/s}$ ), regional transport from the  
262 upwind region contributes the most. Li et al. (2015) found that local emission ( $\sim 50\%$ ) in Shanghai in January 2013 was the  
263 most significant factor causing pollution. Wang et al. (2018) studied with online high-resolution data in December 2014,  
264 and found that local emission had an obvious impact on most pollution sources, while dust emission and coal combustion  
265 had a greater impact on the region.



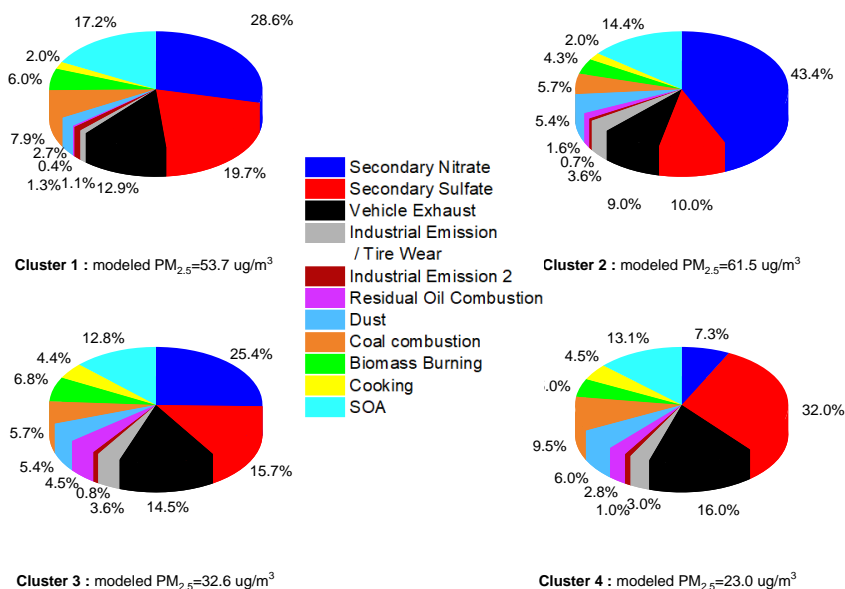
266  
267 **Figure 6. Clustering of air mass trajectories during observation**

268 During the observation period, all the air mass trajectories at the receptor are shown in Figure S4. Fig.6 and table S5  
269 show the clustering results of all air mass trajectories and the average  $\text{PM}_{2.5}$  concentration measured at the sampling time  
270 represented by each cluster. These four clusters accounted for 16.1%, 40.7%, 14.3% and 28.9% of the total trajectory,  
271 respectively. It can be seen from Fig.7 that the composition varies with the source of the air mass. The average concentration  
272 of modeled  $\text{PM}_{2.5}$  of each cluster analyzed by the model was  $53.7\ \mu\text{g}/\text{m}^3$ ,  $61.5\ \mu\text{g}/\text{m}^3$ ,  $32.6\ \mu\text{g}/\text{m}^3$  and  $23.0\ \mu\text{g}/\text{m}^3$ ,  
273 respectively. By comparing the four clusters, nitrate was the most important reason for PM pollution in Shanghai.

274 The effect of pollutant accumulation caused by air mass transport represented by cluster 1 and 2 on the average  $\text{PM}_{2.5}$   
275 concentration is significantly greater than the effect of cluster 3 and 4 air mass transport on  $\text{PM}_{2.5}$ . The average  
276 concentration of  $\text{PM}_{2.5}$  in Cluster 1 is slightly larger than that of Cluster 2. According to the length and source of the  
277 trajectories of the respective clusters, cluster 1 is greatly affected by the urban transmission in North China. Coal



278 combustion, biomass burning, vehicle exhaust and secondary sulfate contribution to  $PM_{2.5}$  concentration are greater than  
279 cluster 2. Cluster 2 mainly represents the pollution caused by the accumulation of  $PM_{2.5}$  concentration by local source  
280 emissions. In addition, the contribution of secondary nitrate to  $PM_{2.5}$  in cluster 2 is much larger than that of cluster 1. The  
281 contribution of secondary source to  $PM_{2.5}$  concentration is as high as 67.8%, and the secondary conversion of local source  
282 emission is more obvious. In clusters 1 and 2, SOA is a source of high contribution to total  $PM_{2.5}$  concentration. Both  
283 regional and local source emissions contain a large amount of organic matter, which is an important component of  
284 secondary source pollution. The dust source is also an important source of pollution caused by local emissions leading to  
285 atmospheric  $PM_{2.5}$  pollution.



286  
287 **Figure 7. The percentage of sources under different air mass clusters.**

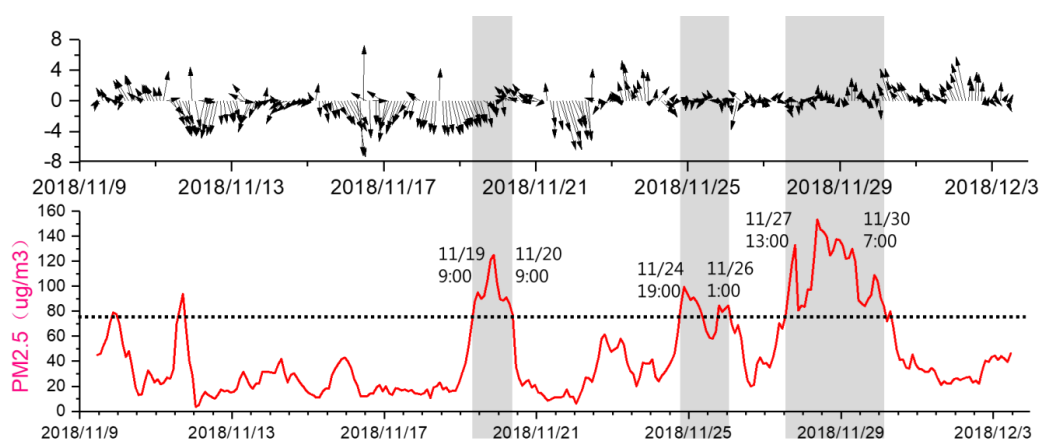
288 Under cluster 3 and 4,  $PM_{2.5}$  concentrations are relatively lower. Their biggest difference is the contribution of  
289 secondary sulfate and secondary nitrate in cluster 3 and cluster 4. Under the influence of the northern air mass transport,  
290 the proportion of secondary sulfate in cluster 4 is much larger than that of secondary nitrate, and also greater than the  
291 proportion of secondary sulfate in cluster 3. It indicates that cluster 4 is discharged from coal combustion in winter in  
292 northern China. And cluster 4 is a long-distance air mass transport, nitrogen oxides are more active in the atmosphere, and  
293 secondary nitrate contributes less in cluster 4 than in cluster 3. In general, in the winter, the coal combustion in the north  
294 of China and the biomass burning will affect the increase of  $PM_{2.5}$  concentration in Shanghai under the action of air mass



295 movement. The accumulation of pollutants caused by local source emissions in Shanghai is also an important cause of  
296  $PM_{2.5}$  pollution in winter.

### 297 3.1.3. Source contribution under different episodes

298 In order to better understand the source composition characteristics of atmospheric particulates during pollution  
299 ( $PM_{2.5} > 75 \mu\text{g}/\text{m}^3$ ), we selected three time periods for further analysis,  $PM_{2.5}$  concentration in the three periods is over  
300  $75 \mu\text{g}/\text{m}^3$  continuously or most of the time, as shown in Fig.8 (shaded area). The first episode (EP1) took place from 9 a.m.  
301 to 9 a.m. on November 19, 2018, and lasted 24 hours. The second episode (EP2) took place between 19 p.m. on November  
302 24 and 1 p.m. on November 26, 2018, during which the  $PM_{2.5}$  concentration decreased, but soon began to rebound. The  
303 third episode (EP3) lasts for a long time period, from 13 p.m. on November 27, 2018 to 7 a.m. on November 30, 2018, and  
304 the  $PM_{2.5}$  average concentration was the highest among the three episodes. It is worth noting that the pollution episode that  
305 occurred from November 9 to 12 was not selected because the concentration of  $PM_{2.5}$  was only over  $75 \mu\text{g}/\text{m}^3$  for a few  
306 hours.



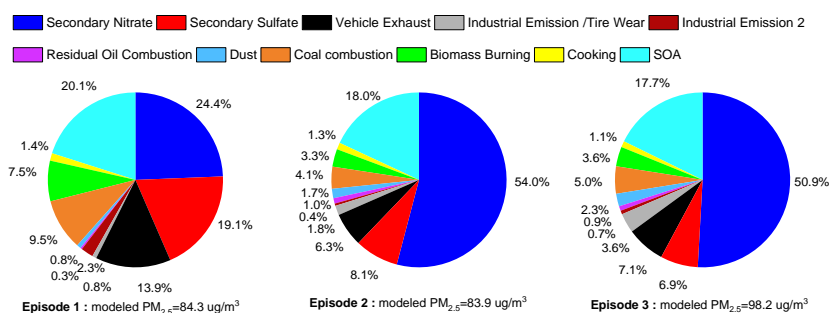
307  
308 **Figure 8. Pollution episodes and its  $PM_{2.5}$  concentration level**

309 The chemical characteristics of the selected three episodes are shown in Figure S5. It can be seen that the percentage  
310 of each component of  $PM_{2.5}$  in the total  $PM_{2.5}$  under three episodes has little difference, indicating that the component will  
311 not change much in a short time period. By analyzing the sources of  $PM_{2.5}$  in the three selected periods, it is found that the  
312 sources of  $PM_{2.5}$  do not follow this rule, as shown in Fig.9. To better understand the influence of regional sources on factors  
313 analyzed by PMF model, using the NOAA HYSPLIT model (<https://ready.arl>) for the three episodes, the 36-hour duration  
314 backward trajectory of the 100-meter AGL was calculated. 0.5 global data assimilation system meteorological data was





315 deployed every 6 hours.



316

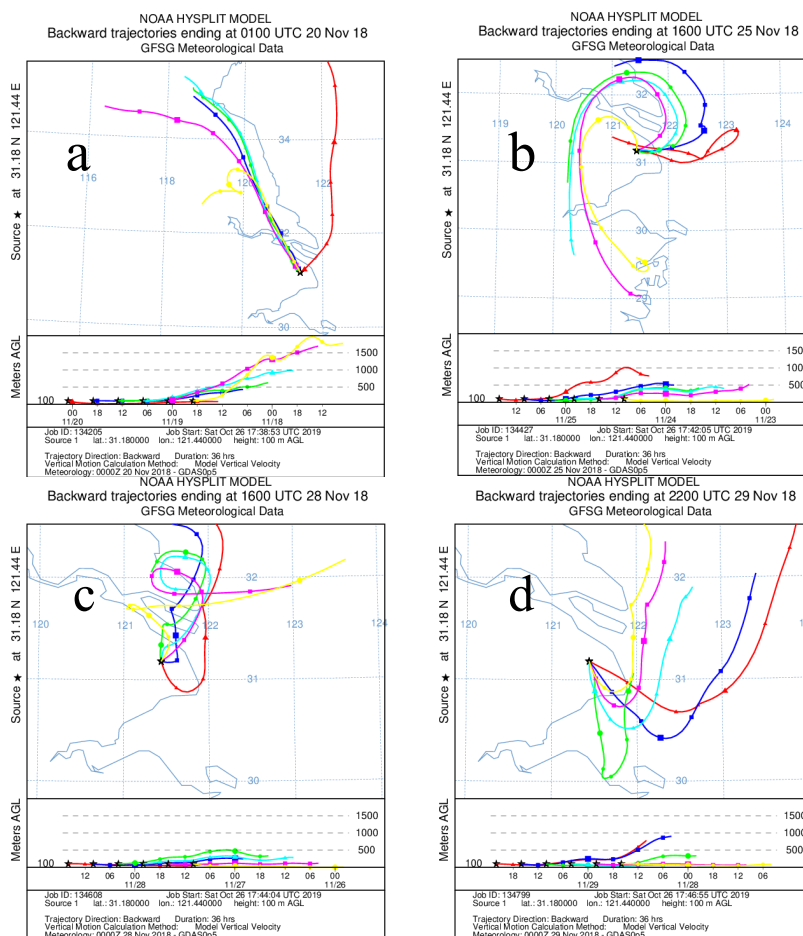
317 **Figure 9. Source contributions under different episodes.**

318 Combining the trajectories of the three episodes (EP1: a; EP2: b; EP3: c& d, Fig.10), the process from pollution  
319 occurrence to pollution dissipation is a process that centers around the monitoring site, and the air mass entering the  
320 monitoring point from the north turns clockwise from the east to the south and enters the monitoring area. And with the  
321 increase of air mass movement in the vertical direction.

322 The average PM<sub>2.5</sub> concentrations observed during the three episodes were EP1: 96.2 μg/m<sup>3</sup>, EP2: 79.8μg/m<sup>3</sup>, and  
323 EP3: 109.1μg/m<sup>3</sup>, EP3>EP1>EP2. Generally speaking, PM<sub>2.5</sub> concentrations are highest when the airflow originates from  
324 the mainland under prevailing northerly winds. When easterly and southerly winds prevail, the PM<sub>2.5</sub> concentration  
325 observed under the influence of oceanic air mass is lower than that of air mass originating from the north. EP3 is greatly  
326 affected by the transition air mass, and the diffusion of adverse pollutants caused by the weak air flow in the vertical  
327 direction and small local wind speed leads to the accumulation of pollutants, resulting in the highest concentration of PM<sub>2.5</sub>.  
328 EP2 is mainly affected by the clean air flow from the south and some ocean air masses, and the vertical movement of the  
329 existing air flow is greater than EP3. Compared with EP2 and EP3, EP1 has a greater contribution to secondary sulphate  
330 factor under the influence of the northern continental air mass, which was close to the study of Hua et al. (2018) on the  
331 source analysis of PM<sub>2.5</sub> in Beijing area. Additionally, secondary sulfate factor may also be affected by primary emission  
332 of coal combustion. Under the influence of the air quality of marine air mass and transition air mass, EP2 and EP3 show  
333 considerable contribution of secondary nitrates (EP2: 54.0% and EP3: 50.7%), while when the land air mass is dominant,  
334 the contribution rate is much lower (EP1: 24.1%). The contribution of biomass burning and coal combustion source factors  
335 show a changing pattern similar to that of secondary sulfate factors, the average contribution is the highest under the  
336 influence of northern air mass, followed by transitional and marine air mass. Under the influence of the southern air mass,  
337 the contribution of biomass burning and coal combustion source factors is the smallest, while the dust source is more



338 affected by local and short-distance air mass transport.



339  
340 **Figure 10.** The backward trajectory by each episode.

341 In EPI, SOA is the largest contributor to the combined effects of anthropogenic and biogenic sources (19.8%), mainly  
342 affected by the secondary conversion of OM carried by long-distance air mass from the north, while vehicle exhaust is  
343 mainly affected by the continental air mass, the secondary conversion is not obvious, and other factors have little effect. In  
344 general, due to differences in energy structure and production and living habits, biomass burning and coal combustion  
345 sources are greatly affected by airflow from the north, which indirectly affects the proportion of secondary sulfate and  
346 secondary nitrate in  $PM_{2.5}$ . Air mass from the south and ocean is cleaner than air mass from the north.  $PM_{2.5}$  pollution is  
347 also affected by the vertical movement of air mass and horizontal wind speed.



### 348 3.2 Impact of organic tracers on source apportionment

349 We also tested the PMF model without including the organic tracers to compare with the base PMF (MM-PMF), which  
350 includes the organic tracers. The input data for PMFt are given in Table S6. In PMFt, eight factors were resolved (see  
351 source profiles in Figure S6), and the three factors, biomass burning, cooking, and SOA could not be extracted due to the  
352 lack of the corresponding organic tracers. The correlation of the common factor contributions for each factor between PMFt  
353 and MM-PMF is shown in Table 3. Generally, the eight common factors, except for secondary sulfate and vehicle exhaust,  
354 the other six factors correlated well between the two runs ( $R = 0.906-0.993$ ), indicating the robustness of the resolved  
355 factors. The secondary sulfate adds more organic matter (PAHs, organic acids, etc.) to the MM-PMF factor profile, showed  
356 a moderate correlation ( $R=0.665$ ) between PMFt and MM-PMF.

357 **Table 3. Correlation (R) of common source factors between PMFt and MM-PMF**

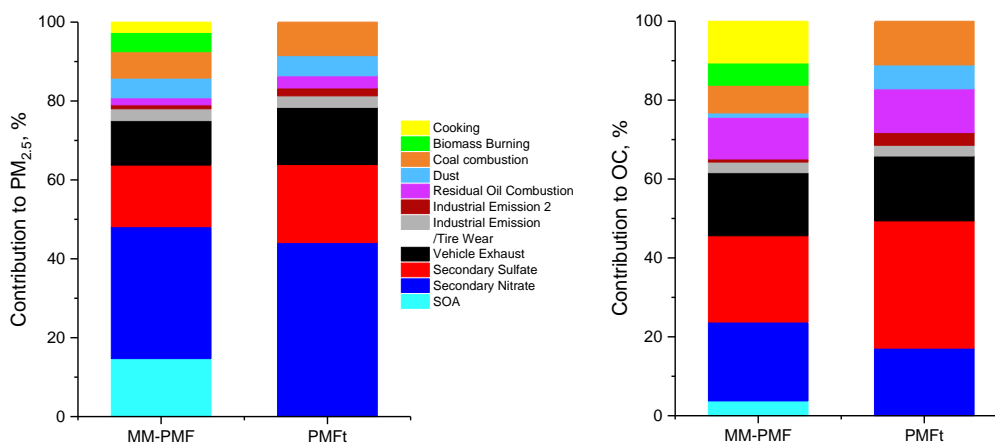
MM-PMF \ PMFt	Secondary Nitrate	Secondary Sulfate	Vehicle Exhaust	Industrial Emission /Tire Wear	Industrial Emission 2	Residual Oil Combustion	Dust	Coal Combustion
Secondary Nitrate	<b>0.906</b>	0.256	0.674	0.388	0.407	-0.036	-0.086	0.458
Secondary Sulfate	0.187	<b>0.665</b>	-0.011	-0.311	0.387	-0.337	-0.377	0.29
Vehicle Exhaust	0.352	-0.265	<b>0.562</b>	0.315	0.321	-0.063	0.094	0.514
Industry / Tire Wear	0.413	-0.225	0.412	<b>0.991</b>	0.151	0.072	0.346	0.236
Industry 2	0.523	-0.033	0.289	0.061	<b>0.983</b>	-0.144	-0.17	0.582
Residual Oil Combustion	-0.064	-0.346	-0.072	0.069	-0.167	<b>0.993</b>	0.264	-0.115
Dust	-0.169	-0.376	-0.196	0.277	-0.181	0.223	<b>0.98</b>	-0.026
Coal combustion	0.573	-0.027	0.436	0.153	0.636	-0.122	-0.013	<b>0.967</b>

358 The factor profiles of PMFt of the 8-factor solution is shown in Figure S6, and the difference of individual factor  
359 contribution to  $PM_{2.5}$  and to OC from MM-PMF and PMFt are shown in Fig. 11. And, among MM-PMF and PMFt results,  
360 the concentrations of reconstructed  $PM_{2.5}$  and OC are shown in Table S7. Compare the factor profiles and contributions of  
361 MM-PMF and PMFt, it can be found that the contribution from the secondary sources changed from ( $29.1 \mu\text{g}/\text{m}^3$ ) 63.8%  
362 of MM-PMF to ( $28.5 \mu\text{g}/\text{m}^3$ ) 63.9% of PMFt, while SOC changed from ( $2.9 \mu\text{g}/\text{m}^3$ ) 46.1% to ( $3.1 \mu\text{g}/\text{m}^3$ ) 48.9% of  
363 the total OC mass. The change in the factor profile of the secondary nitrate to  $PM_{2.5}$  is not obvious, and the contribution of  
364 secondary nitrate to  $PM_{2.5}$  was greater than that of secondary sulfate. While for OC, the contribution of secondary sulfate  
365 was greater than that of secondary nitrate in the two PMF analysis results. In addition, the source apportionment results  
366 under two scenarios showed that secondary sources accounted for 63.9% and 63.8% of the total mass of  $PM_{2.5}$  in PMFt  
367 and MM-PMF, respectively.



368 With the addition of organic tracers, contribution from vehicle exhaust dropped from 14.5% to 11.3% of MM-PMF,  
369 the correlation (R) of the vehicle exhaust between MM-PMF and PMFt was only 0.562 (Table 3), which is mainly because  
370 organic matters were added to the vehicle exhaust factor of MM-PMF, and the factor contribution time series diagram has  
371 changed. There was no significant change in the contribution of vehicle exhaust to OC.

372 The contribution of industrial emission 2 and residual oil combustion sources to PM<sub>2.5</sub> mass changed from 2.0% and  
373 3.1% in PMFt to 1.0% and 1.8% in MM-PMF. This is mainly because OC shifted from these two factors to the newly added  
374 source of MM-PMF. Due to the transfer of OC and other elements (Ca, and Zn, etc.) in the coal combustion, the proportion  
375 of this factor in PM<sub>2.5</sub> decreased from 8.5% of PMFt to 6.7% of MM-PMF. Compared with MM-PMF, the concentration  
376 of OC in industrial emission 2, residual oil combustion and coal combustion in PMFt increased by 0.16, 0.14 and 0.25  
377 µg/m<sup>3</sup>, respectively. Generally, for the eight factors, the factor industrial emission /tire wear and dust were more stable,  
378 contributions of these two factors to total PM<sub>2.5</sub> were relatively small, with little differences between MM-PMF and PMFt  
379 results (3.0% vs 2.9% and 5.0% vs 5.1%), whereas the contribution from dust to the total OC mass changed from (0.10  
380 µg/m<sup>3</sup>) 1.1% of MM-PMF to (0.24 µg/m<sup>3</sup>) 3.8% of PMFt. Compare the difference of individual factor contribution to OC  
381 from MM-PMF and PMFt, POC changed from 53.9% to 51.1% of PMFt of the total OC mass.



382  
383 **Figure 11. Difference of individual factor contribution to PM<sub>2.5</sub> and to OC from MM-PMF and PMFt.**

#### 384 4. Conclusions

385 In this study, an intensive observation campaign was organized in winter to gain more insights into the sources and



386 formation of PM<sub>2.5</sub> in Shanghai, a typical city in the Yangtze River Delta region. PM<sub>2.5</sub> and its chemical components,  
387 including water-soluble inorganic ions, carbonaceous species, trace elements and organic markers (PAHs, sugars, organic  
388 acids, etc.) were measured with 1-h time resolution. By combining comprehensive data sets of chemical species into the  
389 PMF model for source analysis, the average contribution of secondary pollution sources is more than 60%. The MM-PMF  
390 with organic tracers added was further compared with the traditional PMF without organic tracers. MM-PMF further  
391 resolved the source contributions from SOA, biomass burning and cooking factors, which can't be separated without  
392 organic tracers.

393 Comparing the contributions of different sources to OC mass from MM-PMF, it can be seen that SOC and POC  
394 contributed 45.1% and 54.9%, respectively. The SOC associated with secondary nitrate and sulfate factors accounted for  
395 2.68 µg/m<sup>3</sup> (41.3%) on average across all the study. The source of vehicle exhaust contributes the most to POC, in addition,  
396 it is worth noting that the contribution of cooking to PM<sub>2.5</sub> mass only account for 2.6%, but it contribute 10.7% to OC.

397 Comparisons of PM<sub>2.5</sub> source composition under different air quality shows that the secondary nitrate contribution is  
398 much higher when PM<sub>2.5</sub> concentrations are high. The data during the whole observation period were analyzed by backward  
399 trajectory clustering and four types of backward trajectories were analyzed separately. It was found that secondary nitrate  
400 was the main cause of air pollution in Shanghai. In addition, in the absence of pollution, vehicle exhaust sources still make  
401 a significant contribution. In winter, Shanghai area is greatly affected by the air mass from the northern area, which is an  
402 important cause of particulate pollution. In addition, adverse meteorological conditions may also cause the accumulation  
403 of particulate matter, resulting in air pollution.

404

405 *Competing interest.* The authors declare that they have no conflict of interest.

406

407 *Acknowledgement.* This study was financially supported by the National Natural Science Foundation of China (NO.  
408 41875161) and Hong Kong Research Grants Council (16305418). We thank Shanghai Academy of Environmental Sciences  
409 for logistic help with the TAG-GC/MS measurements.

## 410 **References**

- 411 Adachi, K. and Tainosho, Y.: Characterization of heavy metal particles embedded in tire dust, *Environ. Int.*, 30(8), 1009-  
412 1017, 2004.
- 413 Al-Naiema, I. M., Hettiyadura, A. P. S., Wallace, H. W., Sanchez, N. P., Madler, C. J., Cevik, B. K., Bui, A. A. T., Kettler,



- 414 J., Griffin, R. J., and Stone, E. A.: Source apportionment of fine particulate matter in Houston, Texas: insights to  
415 secondary organic aerosols, *Atmos. Chem. Phys.*, 18(21), 15601-15622, <https://doi.org/10.5194/acp-18-15601-2018>,  
416 2018.
- 417 Battelle, (2012). Environmental technology verification report. Retrieved from [http://cooperenvironmental.com/wp-](http://cooperenvironmental.com/wp-content/uploads/2014/09/Xact625_ETVReport-full.pdf)  
418 [content/uploads/2014/09/Xact625\\_ETVReport-full.pdf](http://cooperenvironmental.com/wp-content/uploads/2014/09/Xact625_ETVReport-full.pdf).
- 419 Borai, E. H., El-Sofany, E. A., Abdel-Halim, A. S., and Soliman, A. A.: Speciation of hexavalent chromium in atmospheric  
420 particulate samples by selective extraction and ion chromatographic determination, *Trac-Trend. Anal. Chem.*, 21(11),  
421 741-745, 2002.
- 422 Chang, Y. H., Huang, K., Xie, M. J., Deng, C. R., Zou, Z., Liu, S. D., and Zhang, Y. L.: First long-term and near real-time  
423 measurement of trace elements in China's urban atmosphere: temporal variability, source apportionment and  
424 precipitation effect, *Atmos. Chem. Phys.*, 18(16), 11793-11812, doi:10.5194/acp-18-11793-2018, 2018.
- 425 Chen, J., Liu, G. J., Kang, Y., Wu, B., Sun, R. Y., Zhou, C. C., and Wu, D.: Atmospheric emissions of F, As, Se, Hg, and  
426 Sb from coal-fired power and heat generation in China, *Chemosphere*, 90(6), 1925-1932, 2013.
- 427 Chen, L. W. A.; Watson, J. G.; Chow, J. C.; and Magliano, K. L.: Quantifying PM<sub>2.5</sub> source contributions for the San Joaquin  
428 Valley with multivariate receptor models, *Environ. Sci. Technol.*, 41(8), 2818-2826, 2007.
- 429 Chow, J. C., Watson, J. G., Kuhns, H., Etyemezian, V., Lowenthal, D. H., Crow, D., Kohl, S. D., Engelbrecht, J. P., and  
430 Green, M. C.: Source profiles for industrial, mobile, and area sources in the Big Bend Regional Aerosol Visibility and  
431 Observational study, *Chemosphere.*, 54(2), 185-208, 2004.
- 432 Du, W. J., Zhang, Y. R., Chen, Y. T., Xu, L. L., Chen, J. S., Deng, J. J., Hong, Y. W., and Xiao, H.: Chemical Characterization  
433 and Source Apportionment of PM<sub>2.5</sub> during Spring and Winter in the Yangtze River Delta, China, *Aerosol. Air. Qual.*  
434 *Res.*, 17(9), 2165-2180, 2017.
- 435 Engling, G., Carrico, C. M., Kreidenweis, S. M., Collett, J. L., Day, D. E., Malm, W. C., Lincoln, E., Hao, W. M., Iinuma,  
436 Y., and Herrmann, H.: Determination of levoglucosan in biomass combustion aerosol by high-performance anion-  
437 exchange chromatography with pulsed amperometric detection, *Atmos. Environ.*, 40, S299-S311, 2006.
- 438 Fang, T., Guo, H., Verma, V., Peltier, R., and Weber, R.: PM<sub>2.5</sub> water-soluble elements in the southeastern united states:  
439 Automated analytical method development, spatiotemporal distributions, source apportionment, and implications for  
440 health studies, *Atmos. Chem. Phys.*, 15(20), 11667-11682. doi:10.5194/acp-15-11667-2015, 2015.
- 441 Feng, J. L., Sun, P., Hu, X. L., Zhao, W., Wu, M. H., and Fu, J. M.: The chemical composition and sources of PM<sub>2.5</sub> during  
442 the 2009 Chinese New Year's holiday in Shanghai, *Atmos. Res.*, 118, 435-444, 2012.
- 443 Feng, J. L., Li, M., Zhang, P., Gong, S. Y., Zhong, M. A., Wu, M. H., Zheng, M., Chen, C. H., Wang, H. L., and Lou, S. R.:  
444 Investigation of the sources and seasonal variations of secondary organic aerosols in PM<sub>2.5</sub> in Shanghai with organic  
445 tracers, *Atmos. Environ.*, 79, 614-622, 2013.
- 446 Feng, J. L., Zhang, Y., Li, S. S., Mao, J. B., Patton, A. P., Zhou, Y. Y., Ma, W. C., Liu, C., Kan, H. D., Huang, C., An, J. Y.,  
447 Li, L., Shen, Y., Fu, Q. Y., Wang, X. N., Liu, J., Wang, S. X., Ding, D., Cheng, J., Ge, W. Q., Zhu, H., and Walker, K.:  
448 The influence of spatiality on shipping emissions, air quality and potential human exposure in the Yangtze River  
449 Delta/Shanghai, China, *Atmos. Chem. Phys.*, 19(9), 6167-9183, doi:10.5194/acp-19-6167-2019, 2019.
- 450 Foley, K. M., Roselle, S. J., Appel, K. W., Bhawe, P. V., Pleim, J. E., Otte, T. L., M athur, R., Sarwar, G., Young, J. O.,  
451 Gilliam, R. C., Nolte, C. G., Kelly, J. T., Gilliland, A. B., and Bash, J. O.: Incremental testing of the Community  
452 Multiscale Air Quality (CMAQ) modeling system version 4.7, *Geosci. Model Dev.*, 3, 205-226,  
453 <https://doi.org/10.5194/gmd-3-205-2010>, 2010.
- 454 Griffith, S. M., Huang, X. H. H., Louie, P. K. K., and Yu, J. Z.: Characterizing the thermodynamic and chemical composition  
455 factors controlling PM<sub>2.5</sub> nitrate: Insights gained from two years of online measurements in Hong Kong, *Atmos. Environ.*,



- 456 122, 864-875, 2015.
- 457 Hopke, P. K.: Review of receptor modeling methods for source apportionment, *J. Air Waste Manage.*, 66, 237-259,  
458 <https://doi.org/10.1080/10962247.2016.1140693>, 2016.
- 459 Hu, D., Bian, Q. J., Lau, A. K. H., and Yu, J. Z.: Source apportioning of primary and secondary organic carbon in summer  
460 PM<sub>2.5</sub> in Hong Kong using positive matrix factorization of secondary and primary organic tracer data, *J. Geophys. Res-*  
461 *Atmos.*, 115, D16204, 2010.
- 462 Hua, Y., Wang, S. X., Jiang, J. K., Zhou, W., Xu, Q. C., Li, X. X., Liu, B. X., Zhang, D. W., and Zheng, M.: Characteristics  
463 and sources of aerosol pollution at a polluted rural site southwest in Beijing, China, *Sci. Total. Environ.*, 626, 519-527,  
464 2018.
- 465 Huang, R. J., Zhang, Y., Bozzetti, C., Ho, K. F., Cao, J. J., Han, Y. M., Daellenbach, K. R., Slowik, J. G., Platt, S. M.,  
466 Canonaco, F., Zotter, P., Wolf, R., Pieber, S. M., Bruns, E. A., Crippa, M., Ciarelli, G., Piazzalunga, A., Schwikowski,  
467 M., Abbaszade, G., Schnelle-Kreis, J., Zimmermann, R., An, Z. S., Szidat, S., Baltensperger, U., El Haddad, I., and  
468 Prevot, A. S. H.: High secondary aerosol contribution to particulate pollution during haze events in China, *Nature*,  
469 514(7521), 218-222, 2014.
- 470 Isaacman, G., Kreisberg, N. M., Yee, L. D., Worton, D. R., Chan, A. W. H., Moss, J. A., Hering, S. V., and Goldstein, A.  
471 H.: Online derivatization for hourly measurements of gas- and particle-phase semi-volatile oxygenated organic  
472 compounds by thermal desorption aerosol gas chromatography (SV-TAG), *Atmos. Meas. Tech.*, 7(12), 4417-4429, 2014.
- 473 Jang, M. S., Czoschke, N. M., Lee, S., and Kamens, R. M.: Heterogeneous atmospheric aerosol production by acid-  
474 catalyzed particle-phase reactions, *Science*, 298(5594), 814-817, 2002.
- 475 Jaeckels, J. M., Bae, M. S., and Schauer, J. J.: Positive matrix factorization (PMF) analysis of molecular marker  
476 measurements to quantify the sources of organic aerosols, *Environ. Sci. Technol.*, 41(16), 5763-5769, 2007.
- 477 Jeong, C. H., Wang, J. M., Hilker, N., Debosz, J., Sofowote, U., Su, Y. S., Noble, M., Healy, R. M., Munoz, T., Dabek-  
478 Zlotorzynska, E., Celoz, V., White, L., Audette, C., Herod, D., and Evans, G. J.: Temporal and spatial variability of traffic-  
479 related PM<sub>2.5</sub> sources: Comparison of exhaust and non-exhaust emissions, *Atmos. Environ.*, 198, 55-69, 2019.
- 480 Jimenez, J. L., Canagaratna, M. R., Donahue, N. M., Prevot, A. S. H., Zhang, Q., Kroll, J. H., and Worsnop, D. R.: Evolution  
481 of organic aerosols in the atmosphere, *Science*, 326(5959), 1525-1529, 2009.
- 482 Kanakidou, M., Seinfeld, J. H., Pandis, S. N., Barnes, I., Dentener, F. J., Facchini, M. C., Van Dingenen, R., Ervens, B.,  
483 Nenes, A., and Nielsen, C. J.: Organic aerosol and global climate modelling: a review, *Atmos. Chem. Phys.*, 5, 1053-  
484 1123, 2005.
- 485 Karar, K., Gupta, A. K., Kumar, A., and Biswas, A. K.: Characterization and identification of the sources of chromium,  
486 zinc, lead, cadmium, nickel, manganese and iron in PM<sub>10</sub> particulates at the two sites of Kolkata, India, *Environ. Monit.*  
487 *Assess.*, 120(1-3), 347-360, 2006.
- 488 Lee, S., Liu, W., Wang, Y. H., Russell, A. G., and Edgerton, E. S.: Source apportionment of PM<sub>2.5</sub>: Comparing PMF and  
489 CMB results for four ambient monitoring sites in the southeastern United States, *Atmos. Environ.*, 42(18), 4126-4137,  
490 2008.
- 491 Li, L., An, J. Y., Zhou, M., Yan, R. S., Huang, C., Lu, Q., Lin, L., Wang, Y. J., Tao, S. K., Qiao, L. P., Zhu, S. H., and Chen,  
492 C. H.: Source apportionment of fine particles and its chemical components over the Yangtze River Delta, China during  
493 a heavy haze pollution episode, *Atmos. Environ.*, 123, 415-429, 2015.
- 494 Li, R., Mei, X., Wei, L. F., Han, X., Zhang, M. G., and Jing, Y. Y.: Study on the contribution of transport to PM<sub>2.5</sub> in typical  
495 regions of China using the regional air quality model RAMS-CMAQ, *Atmos. Environ.*, 214, 116856, 2019.
- 496 Lippmann, M., Chen, L. C.: Health effects of concentrated ambient air particulate matter (CAPs) and its components, *Crit.*  
497 *Rev. Toxicol.*, 39(10), 865-913, 2009.



- 498 Liu, B., Song, N., Dai, Q., Mei, R., Sui, B., Bi, X., and Feng, Y.: Chemical composition and source apportionment of  
499 ambient PM<sub>2.5</sub> during the non-heating period in Tai'an, China, *Atmos. Res.*, 170, 23-33, 2016.
- 500 Liu, S. Y. and Liang, X. Z.: Observed diurnal cycle climatology of planetary boundary layer height, *J. Climate*, 23(21),  
501 5790-5809, 2010.
- 502 Masiol, M., Hopke, P. K., Felton, H. D., Frank, B. P., Rattigan, O. V., Wurth, M. J., and LaDuke, G. H.: Source  
503 apportionment of PM<sub>2.5</sub> chemically speciated mass and particle number concentrations in New York City, *Atmos.*  
504 *Environ.*, 148, 215-229, 2017.
- 505 Makkonen, U., Virkkula, A., Mantykentta, J., Hakola, H., Keronen, P., Vakkari, V., and Aalto, P. P.: Semi-continuous gas  
506 and inorganic aerosol measurements at a Finnish urban site: Comparisons with filters, nitrogen in aerosol and gas phases,  
507 and aerosol acidity, *Atmos. Chem. Phys.*, 12(12), 5617-5631, <https://doi.org/10.5194/acp-12-5617-2012>, 2012.
- 508 Mimura, T., Ichinose, T., Yamagami, S., Fujishima, H., Kamei, Y., Goto, M., and Matsubara, M.: Airborne particulate matter  
509 (PM<sub>2.5</sub>) and the prevalence of allergic conjunctivitis in Japan, *Sci. Total. Environ.*, 487(1), 493-499, 2014.
- 510 Nel, A.: Air pollution-related illness: Effects of particles, *Science*, 308(5723), 804-806, 2005.
- 511 Nicolosi, E. M. G., Quincey, P., Font, A., and Fuller, G. W.: Light attenuation versus evolved carbon (AVEC) – A new way  
512 to look at elemental and organic carbon analysis. *Atmos. Environ.*, 175, 145-153, 2018.
- 513 Norris, G., Duvall, R., Brown, S., and Bai, S.: EPA positive matrix factorization (PMF) 5.0 fundamentals and user guide,  
514 U.S. Environmental Protection Agency, Washington, DC, EPA/600/R-14/108 (NTIS PB2015-105147), 2014.
- 515 Paatero, P. and Tapper, U.: Positive matrix factorization: A nonnegative factor model with optimal utilization of error  
516 estimates of data values, *Environmetrics*, 5, 111-126, 1994.
- 517 Pant, P. and Harrison, R. M.: Estimation of the contribution of road traffic emissions to particulate matter concentrations  
518 from field measurements: A review, *Atmos. Environ.*, 77, 78-97, 2013.
- 519 Qiao, L. P., Cai, J., Wang, H. L., Wang, W. B., Zhou, M., Lou, S. R., Lou, S. R., Chen, R. J., Dai, H. X., Chen, C. H., and  
520 Kan, H. D.: PM<sub>2.5</sub> constituents and hospital emergency-room visits in Shanghai, China, *Environ. Sci. Technol.*, 48(17),  
521 10406-10414, 2014.
- 522 Qiao, T., Zhao, M. F., Xiu, G. L., and Yu, J. Z.: Simultaneous monitoring and compositions analysis of PM<sub>1</sub> and PM<sub>2.5</sub> in  
523 Shanghai: Implications for characterization of haze pollution and source apportionment, *Sci. Total. Environ.*, 557, 386-  
524 394, 2016.
- 525 Ramanathan, V.; Crutzen, P. J.; Kiehl, J. T.; Rosenfeld, D. *Atmosphere - Aerosols, climate, and the hydrological cycle*,  
526 *Science*, 294 (5549), 2119-2124, 2001.
- 527 Shu, L., Wang, T. J., Xie, M., Li, M. M., Zhao, M., Zhang, M., and Zhao, X. Y.: Episode study of fine particle and ozone  
528 during the CAPUM-YRD over Yangtze River Delta of China: Characteristics and source attribution, *Atmos. Environ.*,  
529 203, 87-101, 2019.
- 530 Sofowote, U. M., Rastogi, A. K., Deboz, J., and Hopke, P. K.: Advanced receptor modeling of near-real-time, ambient  
531 PM<sub>2.5</sub> and its associated components collected at an urban-industrial site in Toronto, Ontario. *Atmos. Pollut. Res.*, 5(1),  
532 13-23, 2014.
- 533 Song, Y., Zhang, Y. H., Xie, S. D., Zeng, L. M., Zheng, M., Salmon, L. G., Shao, M., and Slanina, S.: Source apportionment  
534 of PM<sub>2.5</sub> in Beijing by positive matrix factorization, *Atmos. Environ.*, 40, 1526-1537, 2006
- 535 Sun, Y. L., Zhuang, G. S., Tang, A. H., Wang, Y., and An, Z. S.: Chemical characteristics of PM<sub>2.5</sub> and PM<sub>10</sub> in haze-fog  
536 episodes in Beijing, *Environ. Sci. Technol.*, 40(10), 3148-3155, 2006.
- 537 Ulbrich, I. M., Canagaratna, M. R., Zhang, Q., Worsnop, D. R., and Jimenez, J. L.: Interpretation of organic components  
538 from Positive Matrix Factorization of aerosol mass spectrometric data, *Atmos. Chem. Phys.*, 9, 2891-2918,  
539 doi:10.5194/acp-9-2891-2009, 2009.





- 540 Wang, H. L., Qiao, L. P., Lou, S. R., Zhou, M., Chen, J. M., and Wang, Q.: PM<sub>2.5</sub> pollution episode and its contributors  
541 from 2011 to 2013 in urban Shanghai, China, *Atmos. Environ.*, 123, 298-305, 2015.
- 542 Wang, J., Hu, Z. M., Chen, Y. Y., Chen, Z. L., and Xu, S. Y.: Contamination characteristics and possible sources of PM<sub>10</sub>  
543 and PM<sub>2.5</sub> in different unfunctional areas of Shanghai, China, *Atmos. Environ.*, 68, 221229, 2013.
- 544 Wang, Q. Q., Feng, Y. M., Huang, X. H. H., Griffith, S. M., Zhang, T., Zhang, Q. Y., Wu, D., and Yu, J. Z.: Nonpolar organic  
545 compounds as PM<sub>2.5</sub> source tracers: Investigation of their sources and degradation in the Pearl River Delta, China, *J.*  
546 *Geophys. Res-Atmos.*, 121(19), 11862-11879, 2016.
- 547 Wang, Q. Q., He, X., Huang, X. H. H., Griffith, S. M., Feng, Y. M., Zhang, T., Zhang, Q. Y., Wu, D., and Yu, J. Z.: Impact  
548 of secondary organic aerosol tracers on tracer-based source apportionment of organic carbon and PM<sub>2.5</sub>: A Case Study  
549 in the Pearl River Delta, China, *Acs. Earth. Space. Chem.*, 1(9), 562-571, 2017.
- 550 Wang, Q. Q., Qiao, L. P., Zhou, M., Zhu, S. H., Griffith, S., Li, L., and Yu, J. Z.: Source apportionment of PM<sub>2.5</sub> using  
551 hourly measurements of elemental tracers and major constituents in an urban environment: investigation of time-  
552 resolution influence, *J. Geophys. Res-Atmos.*, 123(10), 5284-5300, 2018.
- 553 Wang, Q. Q., He, X., Zhou, M., Huang, D. D., Qiao, L. P., Zhu, S. H., Ma, Y. G., Wang, H. L., Li, L., Huang, H., Xu, W.,  
554 Worsnop, D., Goldstein, Hai Guo, Jian Zhen Yu: Primary organic aerosol source identification and aging observed  
555 by hourly measurements of organic molecular markers in urban Shanghai, China, under preparation, 2019.
- 556 Wang, Y. J., Li, L., Chen, C. H., Huang, C., Huang, H. Y., Feng, J. L., Wang, S. X., Wang, H. L., Zhang, G., Zhou, M.,  
557 Cheng, P., Wu, M. H., Sheng, G. Y., Fu, J. M., Hu, Y., Russell, A. G., and Wumaer, A.: Source apportionment of fine  
558 particulate matter during autumn haze episodes in Shanghai, China, *J. Geophys. Res-Atmos.*, 119(4), 1903-1914, 2014.
- 559 Williams, B. J., Jayne, J. T., Lambe, A. T., Hohaus, T., Kimmel, J. R., Sueper, D., Brooks, W., Williams, L. R., Trimborn,  
560 A. M., Martinez, R. E., Hayes, P. L., Jimenez, J. L., Kreisberg, N. M., Hering, S. V., Worton, D. R., Goldstein, A. H.,  
561 and Worsnop, D. R.: The first combined thermal desorption aerosol gas chromatograph-aerosol mass spectrometer (TAG-  
562 AMS), *Aerosol. Sci. Tech.*, 48(4), 358-370, 2014.
- 563 Yao, L., Yang, L., Yuan, Q., Yan, C., Dong, C., and Meng, C.: Sources apportionment of PM<sub>2.5</sub> in a background site in the  
564 north china plain, *Sci. Total. Environ.*, 541, 590-598, 2016.
- 565 Yu, Q. Q., Gao, B., Li, G. H., Zhang, Y. L., He, Q. F., Deng, W., Huang, Z. H., Ding, X., Hu, Q. H., Huang, Z. Z., Wang,  
566 Y. J., Bi, X. H., and Wang, X. M.: Attributing risk burden of PM<sub>2.5</sub>-bound polycyclic aromatic hydrocarbons to major  
567 emission sources: Case study in Guangzhou, south China, *Atmos. Environ.*, 142, 313-323, 2016.
- 568 Yuan, Z. B., Yu, J. Z., Lau, A. K. H., Louie, P. K. K., and Fung, J. C. H.: Application of positive matrix factorization in  
569 estimating aerosol secondary organic carbon in Hong Kong and its relationship with secondary sulfate, *Atmos. Chem.*  
570 *Phys.*, 6 (1), 25-34, 2006.
- 571 Zhang, Q., Ning, Z., Shen, Z. X., Li, G. L., Zhang, J. K., Lei, Y. L., Xu, H. M., Sun, J., Zhang, L. M., Westerdahl, D., Gali,  
572 N. K., and Gong, X. S.: Variations of aerosol size distribution, chemical composition and optical properties from roadside  
573 to ambient environment: A case study in Hong Kong, china, *Atmos. Environ.*, 166, 234-243, 2017.
- 574 Zhang, Y. X., Sheesley, R. J., Bae, M. S., and Schauer, J. J.: Sensitivity of a molecular marker based positive matrix  
575 factorization model to the number of receptor observations, *Atmos. Environ.*, 43(32), 4951-4958, 2009a.
- 576 Zhang, Y., Sheesley, R. J., Schauer, J. J., Lewandowski, M., Jaoui, M., Offenberg, J. H., Kleindienst, T. E., and Edney, E.  
577 O.: Source apportionment of primary and secondary organic aerosols using positive matrix factorization (PMF) of  
578 molecular markers, *Atmos. Environ.*, 43(34), 5567-5574, doi:10.1016/j.atmosenv.2009.02.047., 2009b.
- 579 Zhao, M. F., Huang, Z. S., Qiao, T., Zhang, Y. K., Xiu, G. L., and Yu, J. Z.: Chemical characterization, the transport  
580 pathways and potential sources of PM<sub>2.5</sub> in Shanghai: Seasonal variations, *Atmos. Res.*, 158, 66-78, 2015.
- 581 Zhao, M. J., Zhang, Y., Ma, W. C., Fu, Q. Y., Yang, X., Li, C. L., Zhou, B., Yu, Q., and Chen, L. M.: Characteristics and



- 582 ship traffic source identification of air pollutants in China's largest port. *Atmos. Environ.*, 64, 277-286, 2013b.
- 583 Zhao, Y. L., Kreisberg, N. M., Worton, D. R., Teng, A. P., Hering, S. V., and Goldstein, A. H.: Development of an in situ
- 584 thermal desorption gas chromatography instrument for quantifying atmospheric semi-volatile organic compounds,
- 585 *Aerosol. Sci. Tech.*, 47(3), 258-266, 2013a.
- 586 Zhou, H., Hopke, P. K., Zhou, C. L., and Holsenc, T. M.: Ambient mercury source identification at a New York State urban
- 587 site: Rochester, NY, *Sci. Total. Environ.*, 650, 1327-1337, 2019.